41 p.

N 64-15535
CODE-1
CR-55580

◆ VIDYA

RESEARCH   **DEVELOPMENT**

1450 PAGE MILL ROAD, PALO ALTO, CALIFORNIA

A DIVISION OF [Itek] CORPORATION

SECOND QUARTERLY PROGRESS REPORT

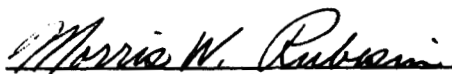STUDY TO EVALUATE EXISTING RE-ENTRY AND OTHER
FLIGHT TEST DATA

This report covers the period June 12, 1963
through September 13, 1963

NASA Contract No. NAS7-216
Vidya Project No. 9058

Prepared by: _W. A. Fleming, Jr._
W. A. Fleming, Jr.
Manager, Reentry Section

Approved by: _M. W. Rubesin_
M. W. Rubesin, Manager
Thermodynamics Department

V I D Y A

A DIVISION OF [Itek] CORPORATION

1450 PAGE MILL ROAD • PALO ALTO, CALIFORNIA
TEL: DAVENPORT 1-2455   TWX: 415 492-9270

TABLE OF CONTENTS

LIST OF FIGURES

LIST OF SYMBOLS

a_1 a constant, $°F/sec^2$

a_2 a constant, $°F/sec^3$

b_n $\dfrac{\pi^2 \alpha (2n + 1)^2}{4l^2}$

$c*$ local sound speed, ft/sec

E distance from thermocouple to heated surface, ft

k thermal conductivity, Btu/ft-sec-$°F$, or, an integer

l thickness, ft

n an integer

p pressure, lb/ft^2

q heat-transfer rate, Btu/ft^2-sec

r body radius, ft

R thermocouple void radius, ft, radial distance from polar coordinate origin, ft

s arc length from stagnation point, ft

t time, sec

u velocity, ft/sec

x thermal diffusivity, ft/sec^2

β $\dfrac{d \ln P}{d \ln \xi}$

ξ $\displaystyle\int_0^s \rho_w \mu_w u_e r^2 \, ds$

ρ density, lb/ft^3

μ viscosity, lb/ft-sec

Subscripts

c   at the thermocouple

e   at the boundary-layer edge

s   at the heated surface

w   at the wall

STUDY TO EVALUATE EXISTING RE-ENTRY AND OTHER
FLIGHT TEST DATA

1. INTRODUCTION

This report summarizes the work initiated and completed under
NASA Contract No. NAS7-216 (Ref. 1) during the second quarter period
June 12, 1963 through September 13, 1963. (This second quarterly
report gives the present status of data collection, summarizes the
results obtained to date in the supporting studies of data-reduction
and heat-transfer prediction methods, and records the man-hour and
dollar expenditure histories through the end of this reporting
period. In addition, the work planned for the next quarterly period
is indicated.

With the exception of some data for the Polaris AIX series
flights noted in Section 2.1 below, all data and other information
necessary for evaluation of re-entry heat transfer for the flights
listed in Reference 1 were collected during this reporting period.
Work was begun on reducing the re-entry heat-transfer (temperature)
data. Development of a digital computer program for direct solution
of the blunt-body inviscid flow-field problem has progressed to the
point where perfect-gas solutions for continuous curvature bodies
and bodies with sonic corners can be obtained. Representative
results obtained to date using this program are given in Section
2.3.2 and compared with corresponding results given by indirect
and empirical methods. A number of available methods for the pre-
diction of heating from fully developed, attached, laminar and
turbulent boundary layers will be used to provide comparisons with
experimental results obtained in this program. These methods are
presented and briefly discussed in Section 2.3.4. They have, for
the most part, been chosen from the methods originally employed
in design and evaluation of the heat shields to be considered in
this study.

2. WORK UNDERTAKEN - JUNE 12, 1963 THROUGH SEPTEMBER 13, 1963

2.1 Data Collection

Authorizations were received during this reporting period for
access to and acquisition of all data and other information neces-
sary for reduction and interpretation of results for the flights
initially designated for consideration (Ref. 1). To date all the
information necessary has been obtained or is in the process of
being transferred to Vidya. Table I summarizes the status of this
collection process at the end of the second quarter. With the
exception of some of the geometrical information and the nose-shield

temperatures for one of the Polaris flights, all of the necessary information is available. Requests for the data not now available have been made to LMSC and it is expected that it will be transmitted to Vidya within the next month.

In general, the temperature data available are in the form of plots of the original, unsmoothed, commutated, and calibrated telemetry signals. These are readable to within $\pm 5^{\circ}$ F which is an order of magnitude less than the scatter band exhibited by the raw data. Work was begun on smoothing the temperature data in preparation for its utilization in the Vidya data-reduction conduction program. It is expected that heat-transfer data reduction for the Air Force Mark 2 and X-17 flights will be completed during the next reporting period.

2.2 Data-Reduction Methods Studies

Experimental results for heat transfer consist of surface heat-transfer rates or heat-transfer coefficients inferred, in general, from digital computer solutions of the variable thermal property conduction equation corresponding to the heat-shield construction. Initial and boundary conditions are defined using smoothed experimental temperature data. There are a number of potentially important error sources in such a data-reduction procedure. For the relatively thick, high thermal conductivity shields such as those to be considered in this study, the errors may result from the following:

(1) Replacement of the continuous shield materials by the lumped parameter nodal structures used in obtaining numerical, that is, finite-difference solutions.

(2) Replacement of the continuous boundary conditions by conditions defined at discrete points in time.

(3) Replacement of the actual temperature response by smoothed data inferred from the scattered experimental results produced by commutated telemetry signals.

(4) Distortion of the shield thermal response from that assumed in the digital conduction solution because of the existence of thermocouple inserts and pressure taps in the actual shield.

(5) Uncertainties in the thermophysical properties of the shield materials and in the contact resistances between materials.

Of these factors, the first two can be minimized, within the limitations of computational costs by proper selection of nodal and input spacing. The third factor must be evaluated empirically

since there is, to the writer's knowledge, no way of operating on the scattered data that will insure that the smoothed temperature response duplicates that of the actual shield. With regard to the fourth potential error source, some work has been done, Reference 2, to determine the disturbance in shield temperature caused at the thermocouple tip location in the limiting case in which the thermocouple is replaced by a void. These results indicate that, in all cases to be considered in this study, the temperature disturbance in this limit is an order of magnitude less than the temperature data scatter bands experienced. The argument leading to this conclusion is given in Section 2.2.2. Finally, evaluation of the effects of uncertainties in the thermophysical properties can best be handled in the course of evaluating the response of specific shield configurations. This factor will not be discussed further at this time. It will be considered, as appears necessary, in the course of evaluating individual flight test results.

The first three of the above factors were evaluated on an empirical basis for cases covering the ranges of conditions anticipated in the flight tests to be considered in this study. This was done by obtaining a series of one-dimensional, constant thermal-property conduction solutions for a 1-inch-thick copper slab perfectly insulated at one surface. This configuration and material are representative of the heat-sink shield sections employed in all but one of the flights to be considered, Reference 1. Digital computer solution results were compared with the analytical solution for surface heat-transfer rates for this configuration with constant initial temperature and a prescribed heated surface temperature response given by

$$T = a_1 t^2 + a_2 t^3 \tag{1}$$

The coefficients in this equation can be adjusted to cover the anticipated range of maximum surface heat-transfer rates which is from approximately 100 to 1000 Btu/sq ft-sec and the range of heat-pulse duration which is from 5 to 50 seconds, References 3 and 4. The surface heat-transfer rate for the above boundary conditions is

$$\frac{l q_s}{2k} = -\frac{a_1 l^4}{3\alpha^2} + \frac{2a_2 l^6}{5\alpha^3} + \left(\frac{a_1 l^2}{\alpha} - \frac{a_2 l^4}{\alpha^2} \right) t + \frac{3}{2} \frac{a_2^2 l^2}{\alpha} t^2$$

$$+ \sum_{0}^{\infty} \left(\frac{2a_1}{b_n^2} - \frac{6a_2}{b_n^3} \right) e^{-b_n t} \tag{2}$$

where

$$b_n = \frac{\pi^2 \alpha (2n + 1)^2}{4 l^2}$$

2.2.1 Nodal spacing and input intervals

The following cases were considered:

Maximum Surface Heat-Transfer Rate (Btu/ft^2-sec)	Approximate Duration of Heat Pulse (sec)	Number of Nodes	Surface Temperature Input Interval (sec)
131.2	50	15, 10, and 5	1
890.8	5	15, 10, and 5	0.10 and 0.20

The temperature history given by Equation (1) was used to define the surface temperature at the discrete input points and linear interpolation was used to determine the surface temperature to be used in actual internal computation steps governed by stability limitations. The results of these calculations were then compared with results given by the corresponding analytical expression for surface heating.

The behavior of the numerical results obtained is typical of those generated in explicit numerical solutions of the conduction equation. Initially large errors (up to 50 percent) in the surface heat-transfer rate damp out within three to six print-out intervals of 1 and 0.1 second in the cases considered here. The error magnitude again increases as the surface heat-transfer rate approaches zero. The results obtained at the time of maximum heat-transfer rate are summarized in Figure 1 which illustrates the effect of the characteristics of the surface temperature response (heat pulse), the nodal spacing used, and the surface temperature input interval. In the higher maximum heat rate case results for the coarser input are apt to be misleading since the errors in the digital solution are alternately high and low in magnitude, while those of the solutions with the finer input are essentially monotonic. Consequently, the error in surface heat-transfer rate is shown for the coarse input case both for the time of maximum surface heat-transfer rate and for the print-out times immediately preceding and following it.

It is concluded from this study that for the relatively short heat pulses associated with the X-17 flights a system of 5 nodes in a direction normal to the primary nose-shield surface is adequate to produce an accuracy of $\pm$ 1 percent in the inferred surface heat-transfer rates near peak heating. For the longer heat pulses associated with the other heat-sink shields to be considered, 15 nodes will be necessary for comparable accuracy. It should be noted that these accuracies are attained using the analytical surface temperature histories as inputs to the conduction solution. The effect of departures from this temperature history in the actual case is discussed below.

2.2.2 Temperature errors and data smoothing

Of the two sources of surface temperature errors in data reduction, items (3) and (4) above, the latter was investigated in Reference 2 for the limit case in which the thermocouple installation is replaced by a cylindrical void. It is shown in Reference 2 that, if the change in surface heat-transfer rate during the response time of the shield material immediately above the void is small (10 percent) relative to the magnitude of surface heat-transfer rate itself, then the departure of the temperature at the thermocouple tip from that that would occur if the thermocouple were not present is given by

$$\delta T_C = q_s \frac{R}{k} f\left(\frac{R}{E}\right)$$

where, for $R/E > 1$, $f(R/E)$ is a linear function. For a 1-inch-thick copper slab, a ratio R/E of unity and thermocouple void radius of 0.02 inch, which are typical of the heat-sink shields considered, thus reduces to

$$\delta T_C = 0.0273 \, q_s$$

The corresponding error at the surface is

$$\delta T_s = 0.0164 \, q_s$$

The maximum magnitude of surface heat-transfer rate anticipated in any of the flights to be considered is (Refs. 3 and 4), approximately, 1500 Btu/ft^2-sec leading to an upper limit of the error in temperature at the thermocouple tip of approximately 41° F. The results indicated above are for steady-state conditions in the terminology of Reference 2, that is, the time at which the point in question is within 10 percent of its asymptotic response value for

a unit step in surface temperature. For times less than this the corresponding errors, again according to Reference 2, are less than those indicated above. This and the fact that the solutions given above are for the limiting case obtained by replacing the thermocouple installation by a void indicate that, in the worst trajectory point to be considered in this study, temperature errors due to the presence of thermocouples are estimated to be no more than approximately 20° F and will range downward to zero as the surface heat-transfer rates decrease from this level. Since the temperature data scatter band is from 100 to 200° F in the heat-sink shield flights tests to be considered in this study, the temperature disturbances caused by the presence of thermocouples are negligible compared with the errors induced as the result of scatter.

As noted above, the scatter bands of the available temperature data range from $\pm$ 50 to $\pm$ 100° F. The problem in utilizing this data is to determine, if possible, the magnitude of the error in surface heat-transfer rates caused by using the scattered temperature data in the data-reduction conduction solution. The customary procedure in processing such data prior to application in the conduction solution is to perform a smoothing operation to reduce the data to a smooth, continuous response curve. Several such smoothing procedures have been proposed and used in the past that range from simple hand fairing of a curve through the data to automatic, usually least squares polynomial, fits. The objective of the automatic smoothing programs is, of course, to eliminate the factor of human judgement in the smoothing process.

Several such smoothing processes were considered for application to the flight test data to be evaluated. The objective of the study was to determine, empirically, with what accuracy one can approximate a known analytical function representing a temperature response by smoothing data generated on the basis of a model of the process by which scatter is produced. The assumptions employed, based to a large extent on the characteristic behavior of the data available, are as follows:

(1) The process by which the data are generated is such as to produce a random scatter in the end results.

(2) The scatter band of a particular data trace is a fixed, constant percentage of the calibrated instrument range.

(3) The temperature response is a smooth, continuous function of trajectory time.

With these assumptions "data" can be generated by starting with a known analytical expression for the temperature, specification of the instrument range and scatter band, and a table of random

numbers, for example, Reference 5. The particular case discussed here used Equation (1) as the known temperature function in the form

$$T = 1.2t^2 - 1.6 \times 10^{-2} t^3$$

which gives a maximum temperature rise of 1000° F at 50 seconds. An instrument range of 1500° F, scatter band of $\pm$ 8 percent of the range, and 1 data point per second were assumed. These assumptions correspond to the worst data observed in any of the experimental results for ballistic vehicle heat shields.

Three smoothing procedures were applied to these data. In all cases the final smoothed temperature curve was constrained to have a zero initial slope which corresponds to conditions at the initiation of re-entry heating for ballistic vehicles as observed in the available temperature data. The first smoothing process consisted of fitting the original data to a least squares cubic over the entire time of the available data. In the second process the data were first smoothed by using a seven point, least squares, walking quadratic to define representative data points at the mid-point of each seven point sample. (This process is described in detail in Ref. 3.) The smoothed data obtained in this manner were then fitted to a least squares cubic over the entire time. Finally, the method developed and used in Reference 6 was employed to determine representative data points which were then fitted to a least squares cubic in the same way as in the other two methods. The argument used in developing this last method is, briefly, that one cannot distinguish changes in the data level to within the scatter band of the data. Consequently, a representation of the true temperature on an interval is obtained simply by averaging all the data points that lie within a scatter band and then moving on and averaging all the data that lie within the next change of the magnitude of a scatter band.

The results obtained with these three methods of smoothing are summarized in Figure 2 which also shows the original curve from which the data were generated. The results shown are indicative of the best that can be expected with these smoothing methods since a choice of a smoothing function corresponding exactly to the form of the actual temperature response function, as was done in developing these results, would be fortuitous. The results show that there is little to choose between direct smoothing of the original data and pre-smoothing using the least squares, walking polynomial method. In this limiting case surface heat-transfer rates inferred from temperatures obtained with either of the first two smoothing methods would differ, during the time of heat flow to the system, only in that the surface heat transfer history would be shifted in time. It is also seen that use of results obtained

with the last method described will produce a surface heat-transfer
history practically identical with that obtained using the original
temperature history except during cooling where the results will
be no worse than those obtained using the better of the first two
smoothing methods.

Based on these preliminary results the procedure being used
in data smoothing is that of the scatter band averaging described
above. Further work planned on the data smoothing problem will
consist of investigating the effect of choosing different polynomial
and other functional forms of the smoothing equation.

2.3 Prediction Methods

Under the flight test conditions to be considered in this study
there is no significant coupling between the boundary layers and
external flow fields during the time of appreciable aerodynamic
heating, that is, $q_s \geq 0.05 q_{s_{max}}$. Consequently, the prediction
problem reduces to definition of the external inviscid flow fields
and, subsequently, application of these results in the heat-transfer
prediction equations. Progress in each of these areas to date is
summarized below. Before describing the prediction work, however,
a brief introduction to a general method of solving nonlinear partial
differential equations is given. This is repeated in greater detail
in the attached appendix. This method was originally applied in
developing a direct method of solution of the blunt-body inviscid
flow problem. In this form it is being applied in this study in
the prediction of inviscid flow fields. As indicated in Section
2.3.4 and the appendix, it is also being considered for application
in obtaining boundary-layer solutions since, based on our study of
the method to date, it appears that it will be as simple to use as
existing prediction methods even though local similarity is not
assumed in obtaining the solutions.

2.3.1 The method of integral relations - application to inviscid
flow-field predictions

The general method of integral relations of A. A. Dorodnitzyn,
Reference 7, is a technique for obtaining solutions of systems of
nonlinear partial differential equations. A description of the
basic ideas employed in the method when applied to equations of
the boundary-layer type is described in the appendix. In this
appendix it is shown that k independent equations for the kth
approximation (i.e., where the boundary layer is divided into k
strips) are derived by introducing k independent smoothing func-
tions into the equations of motion. The original partial differen-
tial equations are reduced to ordinary differential equations by
integrating the equations, multiplied by the smoothing functions,
from the wall to edge of the boundary layer. Hence, k independent
equations result, one for each of the k smoothing functions.

In the solution of the inviscid flow field, the same basic ideas given in the appendix are employed. However, in place of using a system of smoothing functions, the k independent ordinary differential equations are derived by integrating the original equations successively from the body to the upper edge of each of the k strips between the body and the shock wave. Thus, in the first approximation the equations are integrated once between the body and the shock wave. For the second approximation, the equations are integrated first from the body to a line half way between body and shock and second from the body to the shock wave. The further details of describing the resulting integrands by polynomials which depend upon the degree of the approximation follow the description given in Appendix A and, as specifically applied to the inviscid flow-field problem, are given in References 8 and 9.

2.3.2 Digital computer programs and solutions for the inviscid flow fields about blunt bodies

Two complete digital computer programs for solution of the blunt-body inviscid flow field problem using the methods developed initially by Belotserkovskii, Reference 10, from the general formulation of Reference 7, were obtained from Mr. G. H. Hoffman, Lockheed Missiles and Space Company, Huntsville, Alabama. These programs are the result of the work reported in Reference 8 and continued by Mr. Hoffman since that time. In the terminology of the Dorodnitsyn method the programs are for the first and second approximations for computing the flows over blunt two-dimensional and axisymmetric bodies. As received the programs were restricted to perfect-gas flows about bodies generated by conic sections. This latter restriction has been removed since receipt of the programs. The first approximation program is also capable of determining the flow about bodies with a sonic shoulder.

Simply stated the computation proceeds by starting with an assumed shock stand-off distance and integrates the ordinary differential equations resulting from reduction of the continuity and momentum equations. The integration is from the stagnation point in a direction parallel to the body surface and is carried up to the point where the tangential velocity is a specified percentage, usually greater than 80 percent, of the sonic velocity. An iterative procedure is then employed, satisfying the momentum and continuity equations until the shock stand-off distance converges to eight significant figures. At completion of this calculation the solution is extrapolated through the sonic point singularity using a cubic fit to the results at the last three integration points.

There are, of course, very definite limits on the conditions and geometries for which solutions can be obtained. These depend on the geometrical system employed and, in the second and higher approximations, on the computational sequence used in finding the

singularities in the flow between the body and the shock. Work with
the programs to date has been primarily concerned with determining
these limitations and devising methods of eliminating them. These
problems are briefly discussed in the following section.

Samples of results obtained to date are shown in Figure 3.
Conditions for the calculation were chosen to provide a check with
results given in Reference 11. Also shown for comparison are
results for a hemispherically capped cylinder with a sonic shoulder
and the results obtained using the Newtonian approximation. The
agreement with the results for a sphere given in Reference 11 is
excellent. As a matter of interest the IBM 7094 computation time
for the complete sphere was 60 seconds, that for the capped cylinder
was 36 seconds.

2.3.3 Program limitations and modifications

The existing inviscid flow-field computer programs are written
in an R-θ coordinate system. After making several sample runs with
these programs, and taking into account the published work of others
in the field (Refs. 7 and 9), it was found that certain limitations
are inherent in the method in terms of accuracy, Mach number range,
and body shape. All of these limitations are concerned with prac-
tical computational problems, not on basic theoretical considerations.
The various limitations will now be discussed briefly, along with
possible corrections or improvements where applicable.

2.3.3.1 Order of the successive iteration in the second
            approximation

Inherent in the basic method of integral relations applied
to the calculation of inviscid flow fields is an iteration for the
shock stand-off distance in terms of satisfying certain smoothness
requirements on the sonic line. In the second approximation a
successive iteration is required, one for the sonic point on the
body and one for the midway line. Because the present programs
were written for supersonic Mach numbers close to unity, the body
point is iterated on first. For these low Mach numbers, the
coordinate lines θ = constant will intersect the sonic line on
the body before the midway point as shown in the following sketch:

Sonic line

Midway line, second approximation

Body sonic point

R

θ

$$M_\infty \lesssim 2$$
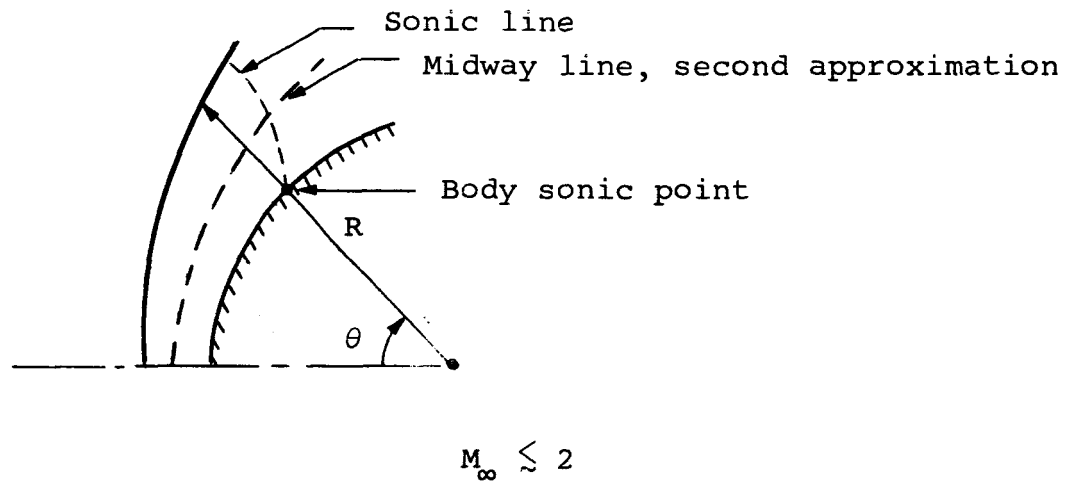
However, for most axisymmetric body shapes, as the Mach number goes above values of about 3, the sonic line bends farther forward so that a θ = constant line will intersect the sonic point on the midway line before the body point. In this latter case, convergence difficulties arise and computational accuracy may be greatly decreased or the computation program simply will not run. Hence, for values of Mach number greater than about 3, the present programs should be reprogramed to reverse the order of the successive iteration scheme.

2.3.3.2 Large Mach number limitation for particular body shapes with the first approximation

In general, it is much easier and much more economical to solve problems employing the first approximation. In terms of acceptable accuracy for the first approximation, it is necessary for the θ = constant lines to be as close to normal to both the body and the shock wave over as much of the computing region as possible. It is obvious that for certain body shapes, particularly at hypersonic Mach numbers where the shock wraps around the body, the R-Q coordinate system is a poor choice. The following sketch shows an example of this.

$$M_\infty > 5$$
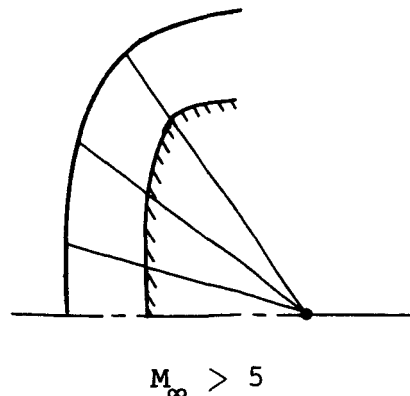
One way to eliminate this problem is to solve the inviscid flow-field equations in an s-n coordinate system (s along the body and n normal to the body). This suggestion, if it leads to acceptable accuracy for the first approximation (a claim made by the Russian workers, see Ref. 12) would also be a solution to the first limitation described above since it would not be necessary to reprogram the second approximation. Reprograming of the first approximation in the s-n coordinate system was initiated during this reporting period in an effort to extend the range of application of the presently available programs.

2.3.3.3 Blunt-cone body shape limitation

When an axisymmetric body is composed of a blunted cone in which the cone angle is near the critical angle (i.e., sonic condition) for the given Mach number, the velocity distribution on the body is as follows:
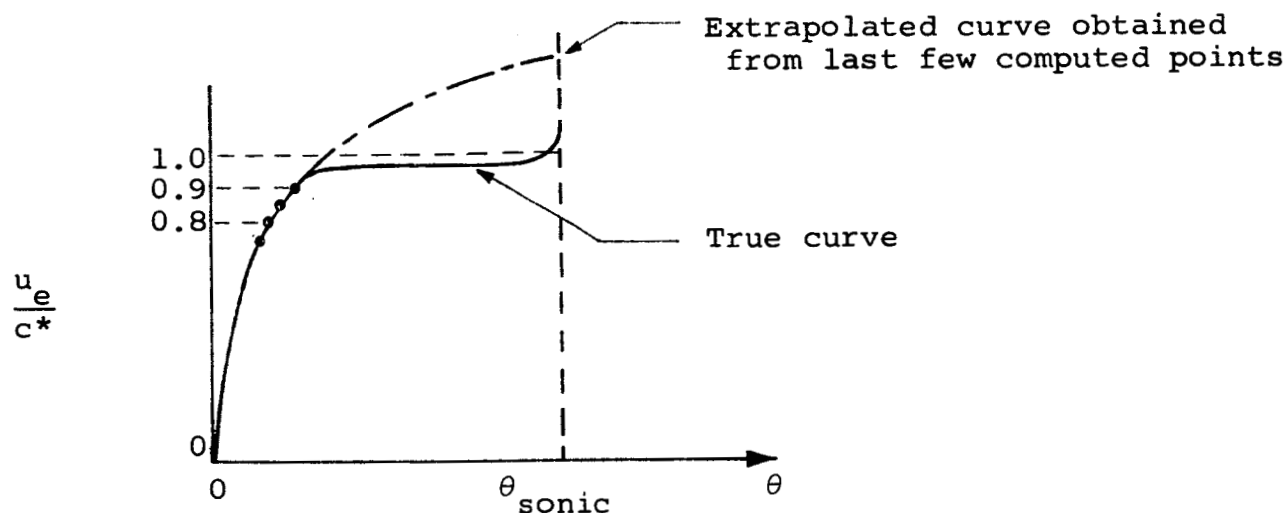
Typical curve for a blunted cone with a sonic corner.

Since the present programs compute to within 5 to 15 percent of the sonic velocity, and then extrapolate to the sonic value, these particular shapes cannot be handled with any reasonable degree of success. At the present time a successful method for overcoming this difficulty has not been found.

2.3.4 Aerodynamic heating prediction methods

Methods for predicting the aerodynamic heating from laminar and fully developed turbulent boundary layers have been chosen, insofar as practical, to include the prediction techniques originally employed in the design and evaluation of re-entry heat shields and to represent a cross section of the many available methods. For stagnation-point heating the flight conditions to be considered are not such as to indicate a distinction between the original prediction form of Fay and Riddell, Reference 13, and the more recent results obtained by Hoshizaki, Reference 14, except as transport properties can be treated parametrically in the method of Reference 13. Both these methods will be employed in predicting stagnation-point heat-transfer rates. The prediction equations to be considered for determining the distribution of aerodynamic heating from laminar boundary layers can all be cast in the same general form. This is shown in Table II which indicates the four methods presently planned for use in comparisons with experimental results. Similarly, three of the four methods to be considered for turbulent boundary layers can be written in a single form as shown in Table III. The remaining turbulent boundary-layer heating prediction method that will be considered is that due to Eckert, Reference 21.

At the present time digital computer programs are being written for the evaluation of the prediction equations shown in Tables II and III. These will incorporate the properties of air in thermochemical equilibrium and will treat the transport properties of air as input parameters. In addition, as indicated above, it is planned to investigate the possibility of using the method of integral relations in the prediction of heating from laminar and turbulent boundary layers. It should be noted in this connection that complete formulations of the systems of ordinary differential equations resulting from application of this method are available through the fourth approximation.

2.4 Man-Hour and Dollar Expenditures

The histories of expenditures of man-hours and dollars through the end of this reporting period are shown in Figure 4. Also shown there are the estimates of these histories made at the beginning of this study.

In evaluating Figure 4 it should be particularly noted that notification of approval of access to the X-17 data was received at Vidya on July 1, 1963, that for the Polaris AIX data on August 7, 1963. Data from the NASA Scout Flight ST-8 were received on August 20, 1963. Since the major cost associated with this study is in the reduction of data, expenditures to date are necessarily below those originally estimated on the assumption of a more or less continuous flow of data for processing. It can be expected

that this situation will be corrected during the next reporting period since nearly all of the data are now available.

3. WORK ANTICIPATED - SEPTEMBER 14, 1963 THROUGH DECEMBER 13, 1963

    The following items represent the work anticipated and estimated degree of completion by the end of the next reporting period:

    (1) Complete collection of all data necessary for data reduction and interpretation. This requires only completion of collection of data for the Polaris AIX flights.

    (2) Complete smoothing of all temperature data in preparation for use in data-reduction conduction calculations.

    (3) Complete data-reduction conduction calculations for as many flights as possible. It is expected that at least three of these can be completed.

    (4) Complete programing of existing laminar and turbulent boundary-layer heat-transfer prediction methods.

    (5) Complete modification of existing ideal-gas inviscid flow field prediction methods. These modifications consist of changing the coordinate and iteration systems in the present programs.

    (6) Complete study of the feasibility of using the method of integral relations in prediction of aerodynamic heating.

    (7) Initiate study of existing data on boundary-layer transition.

REFERENCES

1. NAS 7-216, Study to Evaluate Existing Re-entry and Other Flight Test Data, April 19, 1962.

2. Beck, J. V. and Hurwicz, H.: Effect of Thermocouple Cavity on Heat Sink Temperature, Jour. of Heat Transfer, Feb. 1960.

3. Tellep, D. M. and Hoshizaki, H.: Summary Analysis of X-17 RTV Program, Aerodynamic Heating and Boundary Layer Transistion, Lockheed LMSD 2161, July 2, 1957.

4. Fleming, W. J., Jr., Hines, F. L., and Rindal, R. A.: Development and Evaluation of Re-entry Heating Prediction Methods in the Polaris Fleet Ballistic Missile Program. Trans. 5th Symposium on Ballistic Missile and Space Technology, August 29 - 31, 1960.

5. Reference Data for Radio Engineers, 4th Ed., International Telephone and Telegraph Corp., New York, 1957.

6. Fleming, W. J., Jr., Murphy, J. D., and Hanson, C. W.: Evaluation of Re-entry Heat Transfer Data Obtained in Flight Testing the Air Force Mark 2 Re-entry Vehicle, Vidya Report No. 26, Part I, December 1962.

7. Dorodynitsyn, A. A.: A Contribution to the Solution of Mixed Problems of Transonic Aerodynamics, Adv. in Aero. Sci., Pergamon Press, 1959.

8. Holt, M. and Hoffman, G.: Calculation of Hypersonic Flow Past Spheres and Ellipsoids, ARS Paper No. 61-209-1903, June 1961.

9. Traugott, S. C.: An Approximate Solution of the Direct Supersonic Blunt-Body Problem for Arbitrary Axisymmetric Shape, JAS, vol. 27, no. 5, 1960.

10. Belotserkovskii, O. M.: On the Calculation of Flow Past Axisymmetric Bodies with Detached Shock Waves Using an Electronic Computing Machine, PMM, vol. 24, no. 1, 1960.

11. Inouye, M. and Lomax, H.: Comparison of Experimental and Numerical Results for the Flow of a Perfect Gas About Blunt-Nosed Bodies, NASA TND-1426, September 1962.

12. Belotserkovskii, O. M.: Supersonic Symmetrical Flow of Perfect Gases Around Blunt Bodies, Trans. from J. Computing Math. and Math. Physics, Acad. of Sci., USSR, vol. 2, no. 6, November - December 1962.

13. Fay, J. A. and Riddell, F. R.: Theory of Stagnation Point
     Heat Transfer in Dissociated Air, JAS vol. 25, no. 2, 1958.

14. Hoshizaki, H.: Heat Transfer in Planetary Atmosphere at
     Super-Satellite Speeds, ARS Jour., vol. 25, no. 2, 1962.

15. Lees, L.: Laminar Heat Transfer Over Blunt-Nosed Bodies at
     Hypersonic Flight Speeds. Jet Propulsion, April 1956.

16. Kemp, N. H., Rose, P. H., and Detra, R. W.: Laminar Heat
     Transfer Around Blunt Bodies in Dissociated Air. Jour. Aero.
     Sci., vol. 26, no. 7, July 1959.

17. Burnell, J. A., Goodwin, F. K., Nielsen, J. N., Rubesin, M. W.,
     and Sacks, A. H.: Effects of Supersonic and Hypersonic Air-
     craft Speed Upon Aerial Photography. Vidya Rept. No. 28,
     Oct. 1956.

18. Bromberg, R.: An Approximate Solution of the Boundary Layer
     Equations for Laminar Flow on a Blunt Nose Body of Revolution.
     The Ramo-Wooldridge Corp., April 1955.

19. Rose, P. H., Probstein, R. F., and Adams, M. C.: Turbulent
     Heat Transfer Through a Highly Cooled, Partially Dissociated
     Boundary Layer. AVCO Mfg. Corp. Res. Rep. 14, Jan. 1958.

20. Phillips, R. L.: A Summary of Several Techniques Used in the
     Analysis of High Enthalpy Level, High Cooling Ratio, Turbulent
     Boundary Layers on Blunt Bodies of Revoluation. The Ramo-
     Wooldridge Corp., GM-TM-194, Sept. 1957.

21. Eckert, E. R. G.: Survey of Boundary Layer Heat Transfer at
     High Velocities. WADC TR 59-624, April 1960.

APPENDIX A

DORODNITSYN'S METHOD OF INTEGRAL RELATIONS AND ITS APPLICATION TO COMPRESSIBLE TURBULENT BOUNDARY-LAYER THEORY

The general method of integral relations of A. A. Dorodnitsyn (Ref. 1)[1] is applicable for the solution of systems of nonlinear partial differential equations and was originally applied to the solutions of equations of mixed type (elliptic - hyperbolic) which arise in the solution of supersonic flow over blunt bodies. In 1960 Dorodnitsyn published a paper (Ref. 2) in which he applied his method for finding nonsimilar solutions of incompressible laminar boundary layers. Recently, his method has been used in solving incompressible laminar boundary layers with suction or injection (Ref. 3) and compressible laminar boundary layers including heat transfer to the wall (Ref. 4). The present discussion will describe Dorodnitsyn's method as applied to a general system of partial differential equations. A brief discussion will be given at the end describing how the compressible turbulent boundary-layer equations can be handled.

Perhaps the easiest way to describe the method of integral relations is to compare it to two well-known methods of solving the boundary-layer equations. The first of these is the finite-difference approximation of derivatives.

The finite-difference derivative method for solving partial differential equations is to approximate the derivatives of one

---

[1]References listed at end of this appendix.

variable by an algebraic finite-difference scheme (our present
discussion will be confined to equations with two independent
variables). This method reduces systems of partial differential
equations to systems of ordinary differential equations. For
any finite-difference scheme, numerical accuracy is increased as
the interval (step) size is decreased. For example, a linear
interpolation scheme would be

$$\frac{\partial f}{\partial x} \simeq \frac{f_1 - f_o}{\Delta x}$$

$$\frac{\partial^2 f}{\partial x^2} \simeq \frac{f_2 + f_1 - 2f_o}{(\Delta x)^2}$$

It is well known that, as more and more points are taken and the
interval size Δx approaches zero, the approximation scheme
approaches the true value of the derivative. The basic motivation
of the method, however, is to reduce partial differential equa-
tions to ordinary differential equations.

A second well-known and widely used method of solving the
boundary-layer equations is the Kármán-Pohlhausen integral method.
The motivation behind this technique is also to reduce the problem
to a solution of ordinary differential equations; however, the
basic method employed in the reduction is quite different. In the
Kármán-Pohlhausen method, the partial differential equations are
first integrated over one of the independent variables, resulting
in integro-differential equations. Then, the variation of the

dependent function in the integrated variable is approximated
a priori, permitting evaluation of the integrals. Thus, the
problem reduces to ordinary differential equations in the second
independent variable. Normally, this is done when the variation
of the dependent function is much more rapid in one variable
than the variation in the other variable. The rapid-change vari-
able is then integrated upon. It must be realized, however, that
once the variation in one variable is assumed, no further improve-
ments are possible in correcting the assumed variation within the
framework of the basic method.

Dorodnitsyn's method is also based upon integral approxima-
tions, but there are important differences from the Kármán-
Pohlhausen technique, being in fact an extension of the finite-
difference derivative method. Instead of approximating the
derivatives of one variable by a finite-difference scheme, the
original partial differential equations are integrated (exactly)
with respect to one variable, and then the integrands of the
various integrals are expressed in a finite-difference scheme
by interpolation formulas. The resulting integrals are then
integrated, either analytically or numerically, to yield ordinary
differential equations in the remaining independent variable.
A primary advantage exists, however, in that the finite-difference
interval may be systematically reduced with a corresponding
improvement of accuracy. In the limit, of course, the integrals
become exact.

Dorodnitsyn has shown (Ref. 1) that, for a finite-difference interpolation scheme of a given accuracy, the approximate representation of integrals is more accurate than the representation of derivatives; that is, for a given interpolation formula, the integral of a functional quantity is represented more accurately than its derivative, for a relatively large interval size.

Dorodnitsyn goes one step further than the above description by multiplying the partial differential equations by a suitably chosen smoothing function which permits improved accuracy with large step sizes.

The method of integral relations will now be demonstrated in detail by considering a system of n differential equations with partial derivatives of the following type:

$$\frac{\partial P_i}{\partial x} + \frac{\partial Q_i}{\partial y} = F_i \quad ; \quad i = 1, 2, \ldots , n \tag{1}$$

where

$$P_i = P_i(x,y \; ; \; u_1, u_2, \ldots u_n)$$

$$Q_i = Q_i(x,y \; ; \; u_1, u_2, \ldots u_n)$$

$$F_i = F_i(x,y \; ; \; u_1, u_2, \ldots u_n)$$

$$u_1 = u_1(x,y), \; u_2 = u_2(x,y), \; \ldots u_n = u_n(x,y)$$

where the n-variables $u_1, u_2, \ldots u_n$ are the unknown functions. An important step in the method is to write the equations in divergence form, Equations (1), and for a given problem this must be done initially.

A solution to Equations (1) is sought in the interval $a \leq x \leq b$ (where a may approach $-\infty$ and b may approach $+\infty$) and $c \leq y \leq \delta(x)$.

The given system of Equations (1) are now multiplied by a function of the dependent variables, $f(y)$. At the present, the function $f(y)$ is arbitrary but more will be said about its form later. Next, the Equations (1), multiplied by $f(y)$, are integrated over y from c to $\delta(x)$, yielding

$$\int_c^{\delta(x)} f(y) \frac{\partial P_i}{\partial x} \, dy + \int_c^{\delta(x)} f(y) \frac{\partial Q_i}{\partial y} \, dy = \int_c^{\delta(x)} f(y) \, F_i \, dy \qquad (2)$$

Now, by differentiating the definite integral, it follows that

$$\frac{d}{dx} \int_c^{\delta(x)} f(y) P_i \, dy = \int_c^{\delta} f \frac{\partial P_i}{\partial x} \, dy + \delta' f(\delta) P_i(x, \delta)$$

where $\delta' = d\delta/dx$. The respective functions, $f(\delta)$ and $P_i(\delta)$, are evaluated at the point $y = \delta(x)$.

Also

$$\int_c^{\delta} \frac{\partial \left(f Q_i \right)}{\partial y} \, dy = \int_c^{\delta} f \frac{\partial Q_i}{\partial y} \, dy + \int_c^{\delta} Q_i f' \, dy$$

where $f' = df/dy$. Using these results, it is possible to write Equation (2) in the form

$$\frac{d}{dx} \int_c^{\delta} f P_i \, dy - \delta' f(\delta) P_i(x, \delta) + f(\delta) Q_i(x, \delta) - f(c) Q_i(x, c)$$

$$- \int_c^{\delta} f' Q_i \, dy = \int_c^{\delta} f F_i \, dy \qquad (3)$$

Up to this point only formal mathematics have been used and no approximations have been employed in deriving Equation (3). Now, the basic concepts of the method of integral relations will be introduced.

Consider the function $f(y)$. A <u>system</u> of functions $f_{k,n}(y)$

$$(f_{1,1}), \quad (f_{2,1} \; ; \; f_{2,2}), \quad \ldots \quad , \quad (f_{k,1} \cdots f_{k,k})$$

are chosen such that in the kth group there are contained k mutually independent functions (but in the different groups the functions may coincide). Further, the particular choice of the functions $f_{k,m}$ must be such that convergence of the various integrals of Equation (3) is assured.

Next, the region of interest is divided into k strips as follows:
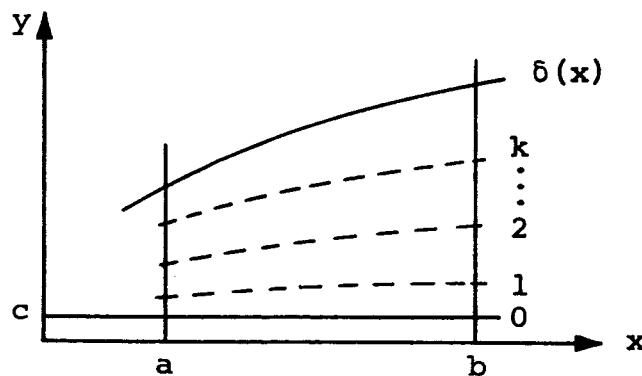
Then, the functions P_i, Q_i, and F_i are approximated with the help of certain interpolation formulas involving the values of P_i, Q_i, and F_i at the boundaries of the strips. For example,

$$P_i(x,y \; ; \; u, u, \ldots u_n) \simeq \sum_{m=0}^{k} P_{i,m}(x) \, Z_m(y) \tag{4}$$

and similarly for Q_i and F_i. Here, $P_{i,m}(x)$ has the value of P_i at the lower edge of the mth strip.

Finally, the resulting ordinary differential equations are found by substituting the interpolation formulas (Eq. (4)) into the integrals and completing the integration. This results in a system of $n \cdot k$ ordinary differential equations (for each of the original n equations, there are now k more equations, one for each $f_{k,n}$). The number of unknown functions (P_i, Q_i, etc.) is $n(k + 1)$ since there are $k + 1$ boundaries for k strips. The physical boundary conditions, for which there are in general n at each boundary (for the original n partial differential equations), provide the remaining equations for the remaining n unknowns. In other words, the method yields

$n(k + 1)$	unknown functions
$n \cdot k$	ordinary differential equations
n	boundary conditions

hence, the problem is closed.

For the particular case at hand, namely, the compressible turbulent boundary-layer equations, we have the following results.

Given equations:

$$u \frac{\partial u}{\partial x} + v \frac{\partial u}{\partial y} = u_1 \frac{du_1}{dx} + \frac{\partial}{\partial y} \left(\epsilon \frac{\partial u}{\partial y} \right) \tag{5}$$

$$\frac{\partial (\rho u)}{\partial x} + \frac{\partial (\rho v)}{\partial y} = 0 \tag{6}$$

$$\epsilon = \epsilon(x,y) \tag{7}$$

Given boundary conditions:

$$y = 0: \quad u = v = 0$$

$$y = \delta(x): \quad u = u_1 \quad , \quad \frac{\partial u}{\partial y} = 0$$

Utilizing Dorodnitsyn's method described above, the equation corresponding to Equation (3) is as follows:

$$\frac{d}{d\xi} \left(\int_0^1 \bar{u}\theta f \, d\bar{u} \right) = \frac{1}{u_1} \frac{du_1}{d\xi} \int_0^1 \theta f'(1 - \bar{u}^2) \, d\bar{u} - \frac{\epsilon(x,0) f'(0)}{\theta_0} - \int_0^1 \frac{\epsilon f''}{\theta} \, d\bar{u} \tag{8}$$

where $\bar{u} = u/u_1$ and

$$\theta = \frac{1}{\partial\bar{u}/\partial\eta}$$

and the $f = f_{k,n}$ are chosen in the form

$$f_{k,m} = (1 - \bar{u})^m \quad ; \quad m = 1, \ldots, k$$

The independent variables ξ and η are related to the original variables x and y through the turbulent analog of the Stewartson-Illingworth transformation as given by Culick and Hill, Reference 5. The function θ is expressed in the kth approximation by an interpolation formula of the form

$$\theta = \frac{1}{1 - \bar{u}}\left(a_o + a_1\bar{u} + \ldots + a_{k-1}\bar{u}^{k-1}\right) \tag{9}$$

and the reciprocal of θ by

$$\frac{1}{\theta} = (1 - \bar{u})\left(b_o + b_1\bar{u} + \ldots + b_{k-1}\bar{u}^{k-1}\right) \tag{10}$$

These approximations for θ and $1/\theta$ automatically satisfy the boundary condition at $y = \delta(x)$, namely, $\partial u/\partial y = 0$. The coefficients $a_o, a_1 \ldots$ and $b_o, b_1 \ldots$ are found from the condition that for

$$\bar{u} = \frac{i}{k} \quad , \quad i = 0, 1, \ldots k - 1$$

the functions θ and $1/\theta$ would equal their exact value; that is, for the kth approximation

$$\bar{u} = 0 \quad , \quad \theta = \theta_o(\xi)$$

$$\bar{u} = \frac{1}{k} \quad , \quad \theta = \theta_1(\xi)$$

$$\bar{u} = \frac{2}{k} \quad , \quad \theta = \theta_2(\xi)$$

$$\vdots$$

$$\bar{u} = \frac{k - 1}{k} \quad , \quad \theta = \theta_{k-1}(\xi)$$

Hence, for the kth approximation, Equation (8) represents k equations in the k unknowns $\theta_o(\xi)$, $\theta_1(\xi)$, ... $\theta_{1-k}(\xi)$. These resulting ordinary, first-order, nonlinear differential equations can be solved numerically by elementary means once $u_1(x)$ and $\epsilon(x,y)$ have been specified.

REFERENCES

1. Dorodnitsyn, A. A.: On a Method of Numerical Solution of Certain Non-linear Problems of Aero Hydrodynamics. Third Union of Math Congress, vol. III, 1956. Akad Nauk SSSR, 1958, pp. 447-453, (in Russian).

2. Dorodnitsyn, A. A.: On a Method of Solution of Laminar Boundary Layers. Prik. Mat. Tekh. Fiz., no. 3, 1960, (in Russian). A shortened version of this paper appears in English under the title: General Methods of Integral Relations and Its Application to Boundary Layer Theory, Advances in Aeronautical Sciences, vol. 3, 1962.

3. Shen-Tsuan, L: Calculation of a Laminar Boundary Layer of an Incompressible Fluid with Suction or Injection. Jour. Computing Math and Math Phyiscs, Academy of Sciences, SSSR, vol. 2, no. 4, 1962, in Russian).

4. Pavlovskii, Y. N.: Numerical Solution of the Laminar Boundary Layer in a Compressible Gas. Jour. Computing Math and Math Physics, Academy of Sciences, SSSR, vol 2, no. 5, 1962, (in Russian).

5. Culick, F. E. C. and Hill, J. A. F.: A Turbulent Analog of the Stewartson-Illingworth Transformation. JAS, vol. 25, no. 4, 1958.

TABLE I.- SUMMARY OF AVAILABLE DATA

Vehicle	Definition of Geometry and Materials	Temperature Data		Pressure Data		Body Motion Data					
						Accelerometer			Rate Gyros		
		Forebody[1]	Afterbody[2]	Forebody[1]	Afterbody[2]	Long.	Lat.	Norm.	Pitch	Yaw	Roll
AF M2 Missile No. 145	X[3]	X	X	X	X	X	X	X	X	X	X
AF X-17 Flight R-2	X	X	NA[4]	X	NA	X	X	X	NA	NA	NA
AF X-17 Flight R-5	X	X	NA	X	NA	X	X	X	NA	NA	NA
AF X-17 Flight R-9	X	X	NA	X	NA	X	X	X	NA	NA	NA
Navy FBM Flight AIX-11	Ordered from LMSC	X	X	NA	NA	X	X	X	X	X	X
Navy FBM Flight AIX-12	Ordered from LMSC	All except nose shield	X	NA	NA	X	X	X	X	X	X
NASA-PARD Flight ST-8	X	X	NA	NA[5]	NA	X	X	X	X	X	X

1. Forebody includes all forward facing surfaces.

2. Afterbody includes all aft facing surfaces.

3. X – material presently available at Vidya.

4. NA – not applicable – vehicle was not instrumented for these measurements.

5. Wind tunnel data available for free stream Mach numbers from 6 to 9.6 and angle of attack up to 25°, NASA TN D-1790, May 1963.

TABLE II.- HEAT-TRANSFER DISTRIBUTIONS FOR FULLY DEVELOPED
LAMINAR BOUNDARY LAYERS

$$\frac{q}{q_{st}} = \frac{1}{\sqrt{2(a+k)}} \left(\frac{R_N}{u_\infty}\frac{du_e}{ds}\bigg|_{s=0}\right)^{1/2} \left\{ \frac{\dfrac{\rho_r \mu_r}{\rho_{st}\mu_{st}}\left(1 - \dfrac{0.1515\,\dfrac{u_e^2}{2Jg}}{H_{st}-H_w}\right)^b \left(\dfrac{r}{R_N}\right)^k \dfrac{\rho_r}{\rho_{st}}\dfrac{\mu_r}{\mu_{st}}\left(\dfrac{u_e}{u_\infty}\right)^a F(\beta)}{\displaystyle\int_0^{s/R_N} \dfrac{\rho_r \mu_r}{\rho_{st}\mu_{st}}\left(\dfrac{r}{R_N}\right)^{2k}\left[1 - \dfrac{0.1515\,\dfrac{u_e^2}{2Jg}}{(H_{st}-H_w)}\right]^b \dfrac{\rho_r \mu_r}{\rho_{st}\mu_{st}}\left(\dfrac{u_e}{u_\infty}\right)^{2a-1} d\dfrac{s}{R_N}} \right\}^{1/2}$$

Theory	Reference	a	b	r	F(β)
Lees	15	1	0	Boundary layer edge	1
Kemp, Rose, and Detra	16	1	0	wall	$\dfrac{1+0.096\sqrt{\beta}}{1.068}$
Rubesin	17	1	2	Reference enthalpy	1
Bromberg	18	1.22	0	Boundary layer edge	1

TABLE III.- HEAT-TRANSFER DISTRIBUTIONS FOR FULLY DEVELOPED
TURBULENT BOUNDARY LAYERS

$$\frac{q_T}{H_{st} - H_w} = \frac{A}{Pr_r^a} \frac{z^b \mu_r^c \rho_r^d u_e^e r^f}{\left[\displaystyle\int_0^s \left(z^b \mu_r^c \rho_r^d u_e^a r^{1+f}\right)^\alpha ds\right]^{1/5}} \left(1 + B \frac{h_D}{H_{st}}\right)$$

Author (Ref.) / Parameter	Rose, Probstein, and Adams (19)	Bromberg I (20)	Rubesin (17)
α	1	1	1
A	0.0301	0.0288	0.0296
B	0.40	0	0
a	2/3	0	2/3
b	0	0	5/4
c	1/4	1/4	1/4
d	1	1	1
e	5/4	1	1
f	9/4	1	1
z	1	1	1
Reference condition r	Boundary-layer edge	Boundary-layer edge	$\dfrac{h_r - H_w}{H_{st} - H_w}$ Reference enthalpy[1]

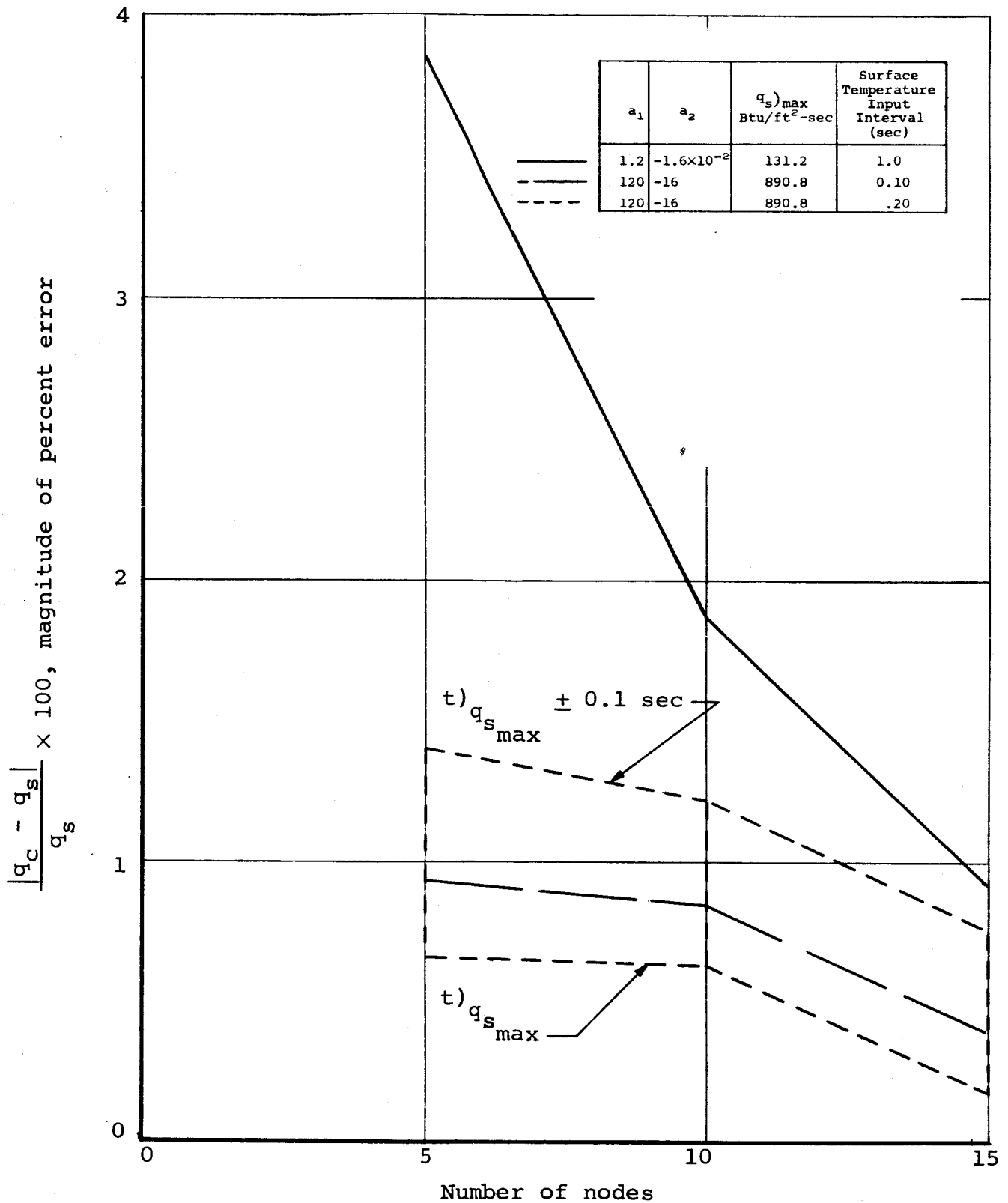[1] $h^* = 0.22H_{st} + 0.28h_o + 0.5H_w$

Figure 1.- Percent error in digital solution for maximum surface heat-transfer rate. (1-inch-thick copper slab perfectly insulated at one surface. Heated surface $\Delta T = a_1 t^2 + a_2 t^3$)
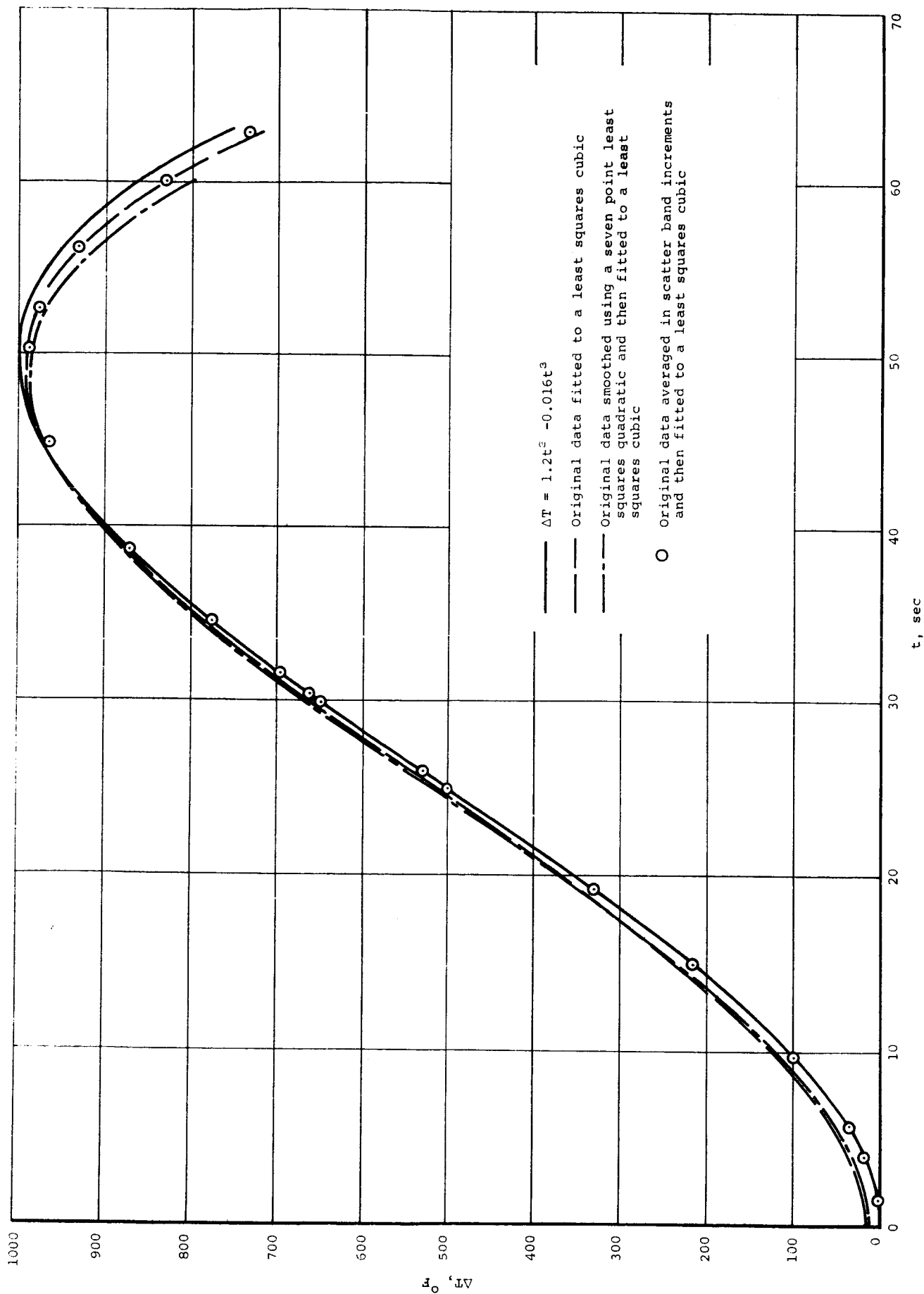
Figure 2.- Comparison of results obtained with three smoothing methods (data sample rate of 1 per second, scatter band ± 120° F).
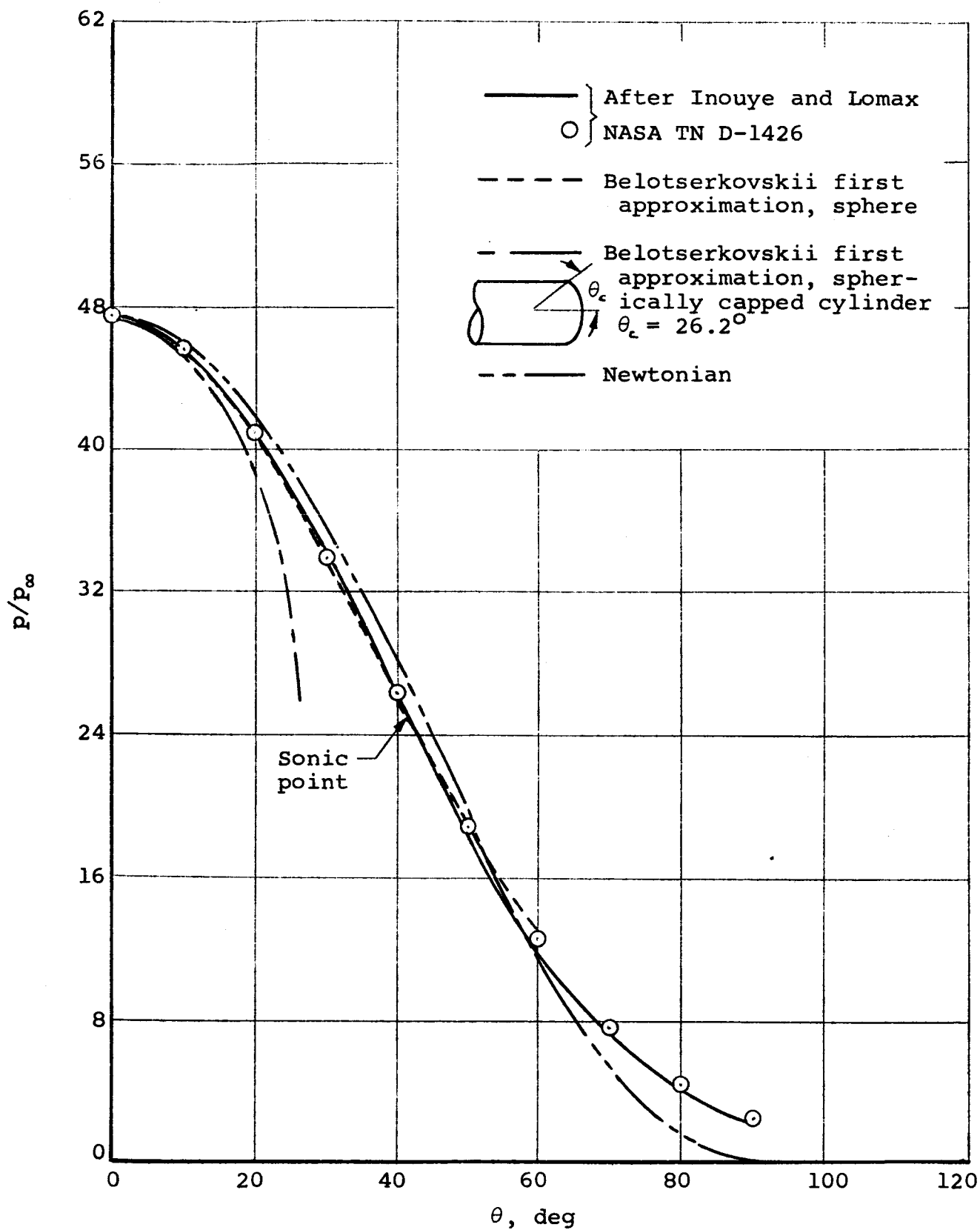
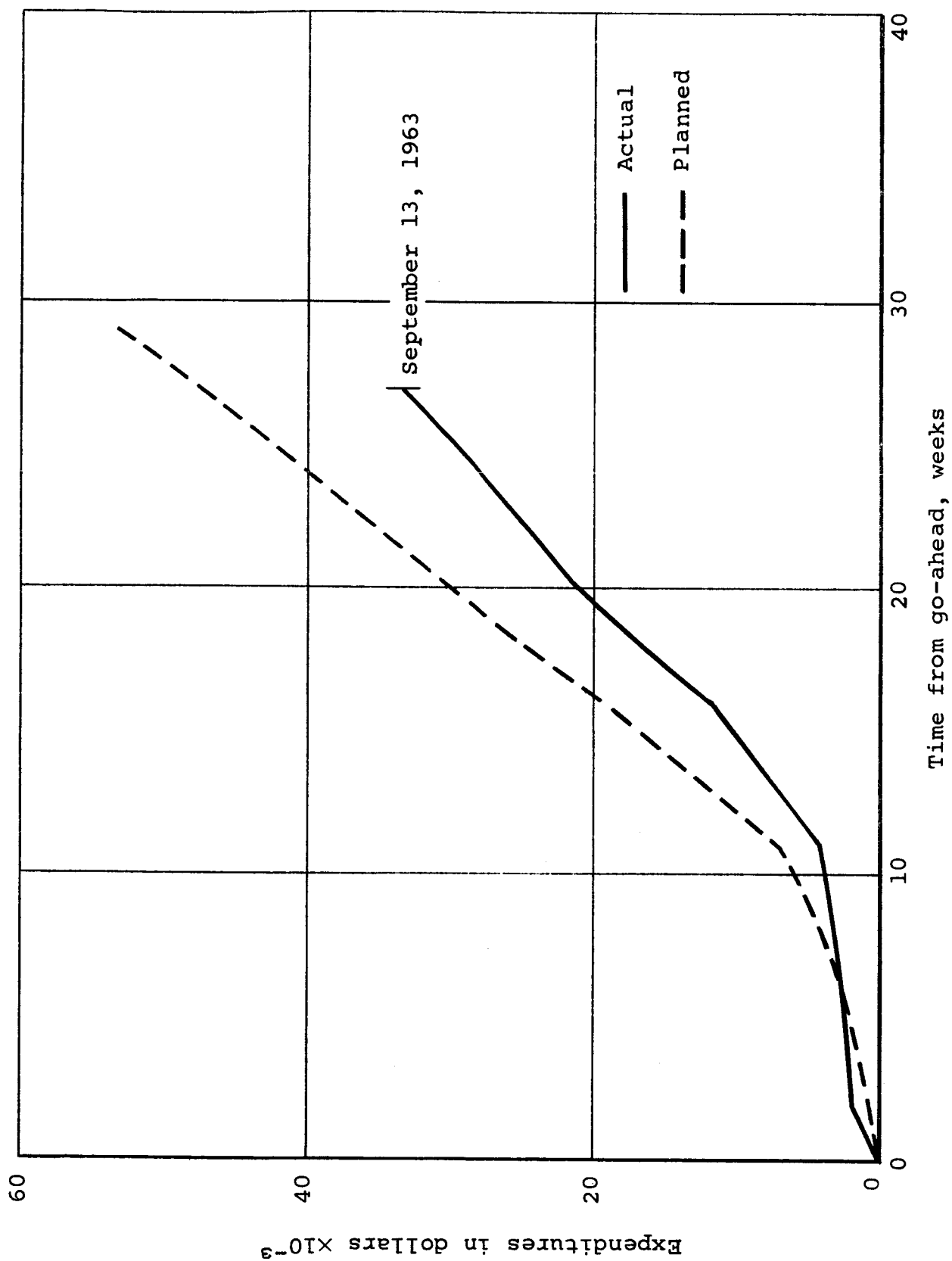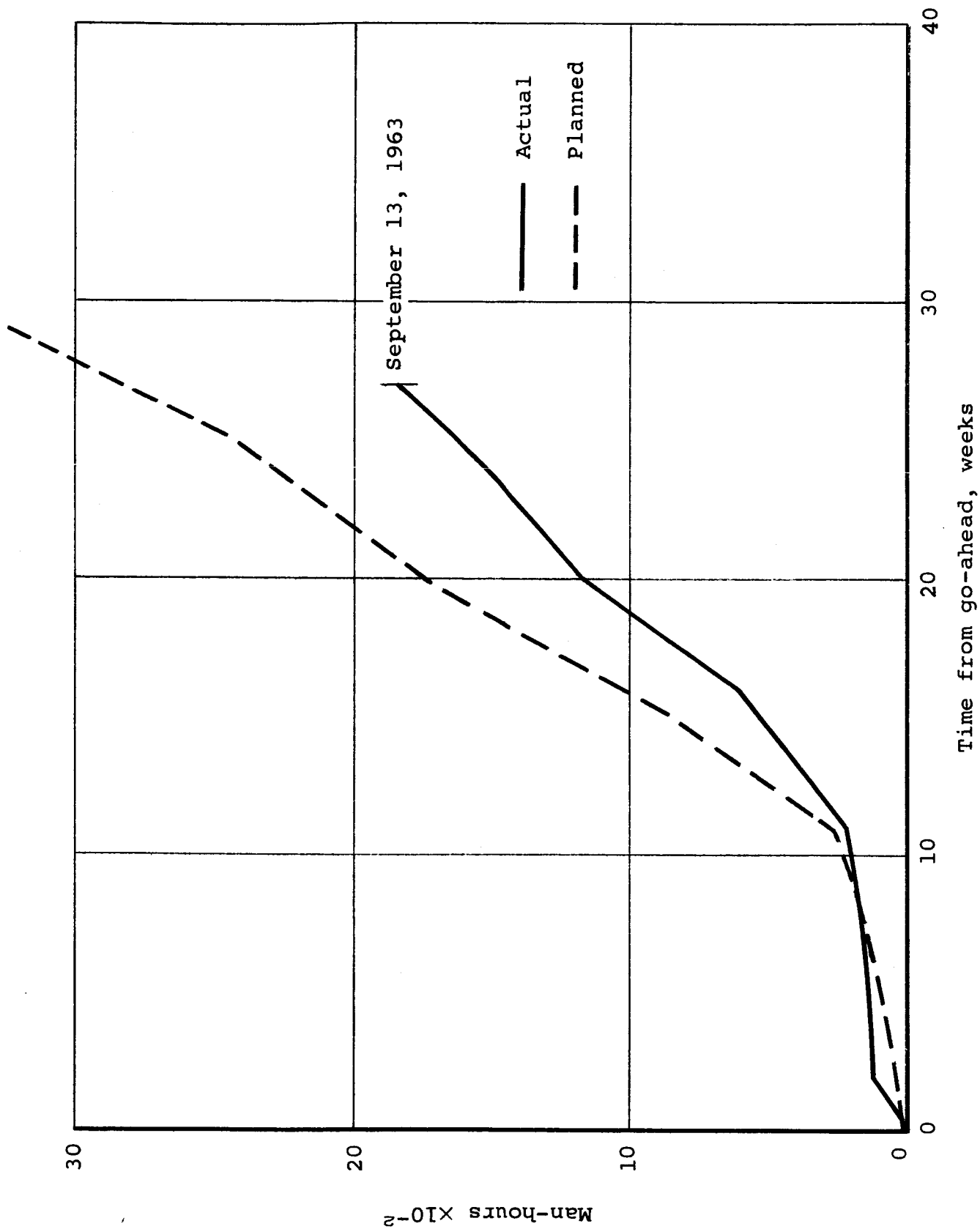Figure 3.- Pressure distribution on a sphere and a spherically capped cylinder $M_\infty = 6.03$, $\gamma = 7/5$.

Time from go-ahead, weeks

September 13, 1963

Actual

Planned

Expenditures in dollars x10⁻³

(a) Dollar expenditures.

Figure 4.- Man-hour and dollar expenditures, NAS7-216.

September 13, 1963

Actual
Planned

Time from go-ahead, weeks

Man-hours $\times 10^{-2}$

(b) Man-hour expenditures.

Figure 4.- Concluded.